EPJ Web of Conferences **192**, 00023 (2018) https://doi.org/10.1051/epjconf/201819200023
QCD@Work 2018

Measurement of hadron form factors at BESIII

Christoph Florian Redmer[1,*] for the BESIII Collaboration

[1]Institut für Kernphysik, Johannes Gutenberg-Universität Mainz, Johann-Joachim-Becher Weg 45, 55128 Mainz, Germany

Abstract. The BESIII experiment, operated at the BEPCII e^+e^- collider in Beijing, has acquired large data sets at center-of-mass energies between 2.0 GeV and 4.6 GeV. One of the key aspects of the physics program of the BESIII collaboration is to test the understanding of QCD at intermediate energies. Applying different experimental techniques, form factors of hadrons are measured. Among these are the pion form factor, as an important input to the $(g-2)_\mu$ puzzle, and the electro-magnetic form factors of nucleons and hyperons in the time-like regime. An overview of the recent results and some ongoing studies at BESIII is provided.

1 Introduction

Hadrons are not point-like. Their spatial extension has been studied e.g. in electron nucleon scattering since the 1960s, and it is still a topic of interest as manifested in the proton radius puzzle [1]. In addition to the size of hadrons, also their internal structure is of interest. It is still not fully understood how the masses of hadrons are generated. While the lightest mesons have masses of the order of 100 MeV and Baryon masses start from approximately 1 GeV, their two or three constituents have masses of only a few MeV, respectively. The difference in mass is assumed to be generated due to the internal dynamics of the hadrons. Observables, which allow to parameterize the structure and the internal dynamics are electromagnetic form factors (EMFF). At the BESIII experiment in Beijing hadron EMFFs are studied to test and enhance the understanding of non-perturbative quantum chromodynamics (QCD), where hadrons and not quarks and gluons are the relevant degrees of freedom.

2 BESIII experiment

The BESIII detector is a magnetic spectrometer [2] located at the Beijing Electron Positron Collider (BEPCII) [3]. The cylindrical core of the BESIII detector consists of a helium-based multilayer drift chamber (MDC), a plastic scintillator time-of-flight system (TOF), and a CsI(Tl) electromagnetic calorimeter (EMC), which are all enclosed in a superconducting solenoidal magnet providing a 1.0 T magnetic field. The solenoid is supported by an octagonal flux-return yoke with resistive plate counter muon identifier modules (MUC) interleaved with steel. The acceptance of charged particles and photons is 93% over 4π solid angle. The charged-particle momentum resolution at 1 GeV/c is 0.5%, and the dE/dx resolution is 6%

*e-mail: redmer@uni-mainz.de

for the electrons from Bhabha scattering. The EMC measures photon energies with a resolution of 2.5% (5%) at 1 GeV in the barrel (end cap) region. The time resolution of the TOF barrel part is 68 ps, while that of the end cap part is 110 ps. The end cap TOF system was upgraded in 2015 with multi-gap resistive plate chamber technology, providing a time resolution of 60 ps [4, 5].

BEPCII provides e^+e^- collisions at center-of-mass energies from 2.0 GeV to 4.6 GeV. It is optimized for the operation at $\sqrt{s} = 3.773\,\text{GeV}$, the peak of the $\psi(3770)$ resonance, where the design luminosity of $10^{33}\,\text{cm}^{-2}\text{s}^{-1}$ has been achieved. The energy dependence of cross sections can be studied in conventional scan measurements in the energy range covered by BEPCII. The method of initial state radiation (ISR) allows to extend the energy range down to the two pion mass threshold. The emission of a photon from the initial state lowers the effective center-of-mass energy $\sqrt{s'} = \sqrt{s - 2\sqrt{s}E_\gamma}$, where E_γ is the energy of the ISR photon. The cross sections measured in this way are radiative cross sections. They are related to the cross section of the process without ISR by the radiator function $H(s, E_\gamma, \theta_\gamma)$, which describes the probability to emit an ISR photon of the energy E_γ at the polar angle θ_γ at a specific $\sqrt{s}$. The relation of radiative and non-radiative cross sections is given by $\frac{d\sigma_{\text{had}+\gamma}}{dm_\gamma} = \frac{2m_{\text{had}}}{s} H(s, E_\gamma, \theta_\gamma)\sigma_{\text{had}}$.

The radiator function produces a characteristic shape in the angular distribution of the ISR photons. Most of the photons are emitted collinear to the lepton beams. The produced hadronic system is boosted in the direction opposite to the photon. Considering the acceptance of the BESIII detector, two different analysis strategies for ISR events can be defined. On the one hand, the hadronic system as well as the ISR photon can be registered in the detector. This case is referred to as "tagged ISR measurement". It allows to measure cross sections from the two-pion mass threshold up to the actual center-of-mass energy of the accelerator. However, with increasing masses of the produced hadronic system, i.e. decreasing photon energies, it is more likely to mistake random signals in the EMC for an ISR photon, leading to a high background contamination. On the other hand, the hadronic system can be measured in the detector, while the ISR photon escapes detection being emitted along the beam axis. By exploiting energy and momentum conservation the photon four-vector can be determined. Requiring its polar angle to be small rejects most of the background events and selects the peaking part of the differential radiative cross section. This scenario is referred to as "untagged ISR measurement". Due to the boost, the acceptance for the hadronic system is limited. The higher the photon energy, i.e. in case of small masses of the hadronic system, the higher is the probability for the final state particles to be emitted close to the beam pipe, where they cannot be registered by a detector. The acceptance of the BESIII detector imposes a threshold of approximately $1\,\text{GeV/c}^2$ on the mass of the hadronic system in an untagged measurement.

Due to the emission of the ISR photon, the radiative process is suppressed by a factor $\frac{\alpha}{\pi}$. In order to perform precision studies, large data samples are required. In the recent years the BESIII collaboration has acquired large data sets of more than $10\,\text{fb}^{-1}$ at center-of-mass energies at and above the $\psi(3770)$ resonance [6, 7]. These are exploited to measure meson and baryon form factors using both, the tagged and untagged ISR methods.

3 Meson form factors

A special interest in meson form factors comes from the anomalous magnetic moment of the muon. There is a long standing discrepancy of more than three standard deviations between the experimental value obtained in a direct measurement [8] and the theory prediction within

the Standard Model (SM) [9]. In order to settle this difference new measurements are performed at FNAL with the aim of a fourfold improvement of the current accuracy [10]. A first result with the accuracy of the previous measurement is expected for spring 2019. Another direct measurement is prepared at J-PARC, using a different approach [11]. The accuracy of the SM prediction is currently completely limited by the hadronic contributions to a_μ. The largest of these contributions comes from leading order hadronic vacuum polarization effects. Due to the asymptotic freedom in the strong interaction, the contribution cannot be evaluated by perturbative means. Besides the recent progress in lattice QCD [12], information from experiment has been used to improve the calculations. The optical theorem relates the leading order vacuum polarization contribution $a_\mu^{hVP,LO}$ to hadronic cross sections measured in e^+e^- collisions. The approach allows to systematically improve the accuracy of $a_\mu^{hVP,LO}$ with high precision measurements of hadronic cross sections. The dispersive integral used to evaluate the cross section also contains a kernel function. Both, the cross sections as well as the kernel function show an energy dependence of $1/s$, putting special emphasis on the cross sections at $\sqrt{s} < 1\,\mathrm{GeV}$. As a consequence, the cross section $\sigma(e^+e^- \to \pi^+\pi^-)$, which includes the production and decay of the ρ resonance, makes up for about 70% of the absolute value of $a_\mu^{hVP,LO}$. To evaluate its uncertainty, the cross sections of higher multiplicities $e^+e^- \to \pi^+\pi^-\pi^0$, $e^+e^- \to \pi^+\pi^-2\pi^0$ and $e^+e^- \to 2\pi^+2\pi^-$ also play an important role.

The cross section $\sigma(e^+e^- \to \pi^+\pi^-)$ has been measured with sub-percent accuracy by the KLOE [13] and BaBar [14] collaborations. However, their results differ by more than 3%, which is reflected in the uncertainty of the evaluation of $a_\mu^{hVP,LO}$. In order to clarify the situation, a new high precision measurement has been performed at BESIII [15]. Based on $2.93\,\mathrm{fb}^{-1}$ of data taken at $\sqrt{s} = 3.773\,\mathrm{GeV}$, the method of tagged ISR has been used to study the cross section of two-pion production at center of mass energies between 600 and $900\,\mathrm{MeV/c^2}$. Due to the similar masses of the final state particles, the radiative production of muon pairs $e^+e^- \to \mu^+\mu^-$ constitutes the dominating background contribution. Combining the information from different sub-detectors, like energy loss in the MDC, energy deposits and shower shapes in the EMC, and the penetration depth in the MUC, an artificial neural network has been trained with Monte Carlo samples to separate effectively muons from pions. Systematic differences between data and simulations have been carefully studied and corrected for. The validity of the corrections has been tested by comparing the muon event yield with the QED prediction as implemented in the Phokhara event generator [16, 17], where an accuracy of 0.5% is claimed. Excellent agreement with the selected data was found.

Finally, the $e^+e^- \to \pi^+\pi^-\gamma_{\mathrm{ISR}}$ signal event yield is corrected for detection efficiency, and is normalized to the integrated luminosity of the data set to obtain the radiative cross section. By correcting for vacuum polarization and FSR effects, and by dividing out the radiator function, the bare cross section, relevant to determine the contribution to $a_\mu^{hVP,LO}$, is calculated. A total uncertainty of the cross section of 0.9% is achieved. The dominating systematic uncertainties are due to the luminosity determination and the knowledge of the radiator function, with 0.5% each.

The BESIII result is compared with previous measurements based on a fit of the pion FF with a Gounaris-Sakurai parameterization, illustrated in Fig. 1. Though systematic deviations can be observed for both, the KLOE results as well as the BaBar results, the value of $a_\mu^{hVP,LO}$ obtained from the evaluation of the dispersive integral agrees nicely with the values obtained by the KLOE collaboration, as shown in Fig. 1. The result of the BESIII measurement is $a_\mu^{\pi\pi,LO}(600-900\,\mathrm{MeV}) = 368.2 \pm 2.5_{\mathrm{stat}} \pm 3.3_{\mathrm{syst}} \cdot 10^{-10}$. It confirms the deviation between the direct measurement and the SM prediction of a_μ to be on the level of more than three standard deviations. Recent dispersive evaluations of compilations of hadronic cross sections [9, 18],

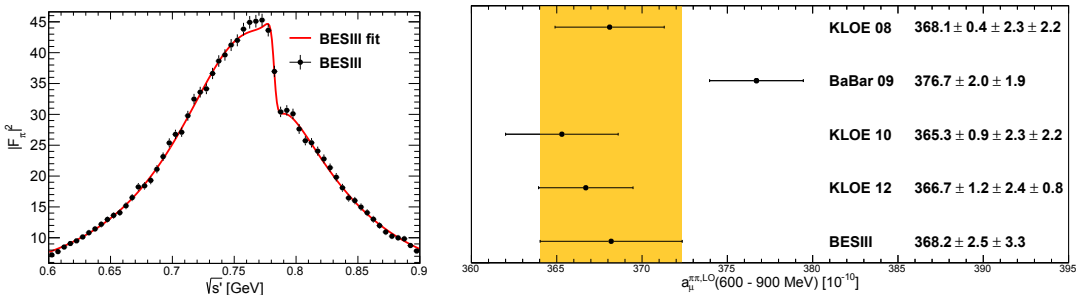

Figure 1. (From Ref. [15]) **left:** Pion FF determined at BESIII with the result of a Gounaris-Sakurai fit. **right:** Comparison of $a_\mu^{\pi\pi,LO}(600-900\,\mathrm{MeV})$ determined at BESIII and by previous experiments.

which include the BESIII result, were able to reduce the uncertainty of the hadronic vacuum contribution to a_μ by more than 20%.

4 Baryon form factors

The number of form factors (FF) of baryons depends on their spin s. Due to their fermionic nature baryons have more than one time-like EMFF, where the number is given by $(2s+1)$. Thus, nucleons and Λ hyperons have two EMFF.

The vertex related to the baryons produced in e^+e^- annihilation can be described as

$$\Gamma^\mu = \gamma^\mu F_1(q^2) + \frac{i\sigma^{\mu\nu}q_\nu}{2M_B}\kappa F_2(q^2), \tag{1}$$

where $F_1(q^2)$ and $F_2(q^2)$ are the Pauli and Dirac FF, respectively. M_B is the mass of the baryon, κ is the anomalous magnetic moment of the baryon, and q^2 is the momentum transfer. Experimentally more convenient is the use of the Sachs FF G_E and G_M, which are linear combinations of the Pauli and Dirac FF:

$$G_\mathrm{E} = F_1(q^2) + \frac{q^2}{4M_B^2}\kappa F_2(q^2) \qquad G_\mathrm{M} = F_1(q^2) + \kappa F_2(q^2) \tag{2}$$

The Sachs FF are EMFFs, describing the charge and magnetic distributions of the baryon. They can be determined by the angular analysis of the differential cross section, which is given as:

$$\frac{\mathrm{d}\sigma^\mathrm{Born}}{\mathrm{d}\Omega} = \frac{\alpha^2\beta^2 C}{4q^2}\left[(1+\cos^2\theta_B^{CM})|G_\mathrm{M}|^2 + \frac{1}{\tau}|G_\mathrm{E}|^2\sin^2\theta_B^{CM}\right], \tag{3}$$

where C is the Coulomb factor, with $C=1$ for neutral and $C = \frac{\pi\alpha}{\beta(1-e^{\pi\frac{\alpha}{\beta}})}$ for charged particles, respectively, and $\beta = \sqrt{1-\frac{1}{\tau}}$ with $\tau = \frac{q^2}{4M_B^2}$.

Assuming the absolute values of the electric and magnetic FF to be equal, information on the effective FF can be extracted from the total cross section of baryon production in e^+e^- annihilation:

$$\sigma_{B\bar{B}}^\mathrm{Born}(q^2) = \frac{4\pi\alpha^2\beta^2 C}{3q^2}\left[|G_\mathrm{M}|^2 + \frac{1}{2\tau}|G_\mathrm{E}|^2\right] \qquad |G_\mathrm{eff}(q^2)| = \sqrt{\frac{\sigma_{B\bar{B}}^\mathrm{Born}(q^2)}{(1+\frac{1}{2\tau})\frac{4\pi\alpha^2\beta^2 C}{3q^2}}} \tag{4}$$

In the following, recent results and selected ongoing studies of nucleon and hyperon EMFF at BESIII are discussed.

4.1 Nucleon form factors

A first measurement of proton EMFFs has been performed at BESIII in 2012 as a scan experiment [19]. At 12 different center of mass energies from 2232.4 MeV to 3671.0 MeV at total integrated luminosity of 157 pb^{-1} has been collected. (Anti-)proton candidates are selected by requiring two oppositely charged tracks per event. By evaluating the energy loss of the tracks in the MDC as well as their associated time of flight, protons are identified. Additional kinematic constraints on the relative opening angles of the tracks in the center-of-mass frame allow to suppress further background. The Born cross section is determined for each energy point by normalizing the background subtracted event yield to the integrated luminosity and reconstruction efficiency, and by correcting for radiative effects. The effective FF extracted from the Born cross section is in agreement with previous measurements, however, the accuracy is improved by approximately 30% due to the BESIII result.

At the three scan point with largest statistics, the differential cross section is studied in order to determine the FF ratio $R = \frac{|G_\mathrm{E}|}{|G_\mathrm{M}|}$. The ratio has been determined in two different ways, using a fit to the angular distributions, and by using the method of moments. Both methods yield compatible results, showing the value of the FF ratio to be consistent with $R = 1$, which supports the assumption used in the extraction of the effective FF. The extracted FF ratio is also in agreement with the BaBar result, however, it is clearly limited by statistics. The result motivated a new, high statistics energy scan at BESIII, which was performed in 2015. The data is still under evaluation.

At the same time, the high statistics samples taken at center-of-mass energies at and above the peak of the $\psi(3770)$ resonance have been exploited to study the proton FF. In total a data set of 7.4 fb^{-1} at energies between $\sqrt{s} = 3.773$ GeV and 4.6 GeV [6, 7] is analyzed using the tagged and untagged ISR methods.

For the tagged ISR method, events with two oppositely charged tracks identified as (anti-)protons and one high energetic photon candidate are selected. Performing a 4C kinematic fit constrained by energy and momentum conservation most background contributions can be suppressed. The dominating background contribution of $e^+e^- \to p\bar{p}\pi^0$ can be suppressed by using a successful 5C kinematic fit with one additional photon in the event as a veto criterion. The additional constraint comes from enforcing the π^0 mass in the fit. In this way, the tagged ISR method allows to study the Born cross section and the effective FF in 31 bins from the $p\bar{p}$ threshold up to 3.0 GeV. In order to extract the FF ratio in an angular analysis with reasonable accuracy, the number of bins is reduced to six.

The untagged ISR method is exploited by selecting events with two oppositely charged tracks, which have been identified as protons. The missing momentum to the $p\bar{p}$ par is calculated and required to have a small polar angle, assuming it is due to a photon that escaped detection along the beam pipe. Correspondingly, the event candidates must yield a small missing mass. With this analysis scheme, the Born cross section of $e^+e^- \to p\bar{p}$ and the effective proton FF can be investigated in 30 bins from $\sqrt{s} = 2.0$ GeV to 3.0 GeV. The angular analysis of the FF ratio is performed in three bins of this mass range.

The preliminary results of the angular analysis of both ISR methods are shown in Fig. 2. The accuracy is competitive with previous measurements. The FF ratios are in agreement with the BaBar result as well as the published BESIII scan measurement [19].

Also the preliminary results on the Born cross section and the effective FF of the tagged as well as untagged ISR methods are shown in Fig. 2. They are consistent with previous measurements. The untagged BESIII result is competitive in its statistical accuracy with the BaBar result, which has been obtained with the tagged ISR methods on a significantly larger data sample. The result clearly demonstrates the advantage of BESIII being able to access the small angle ISR events in the untagged method.

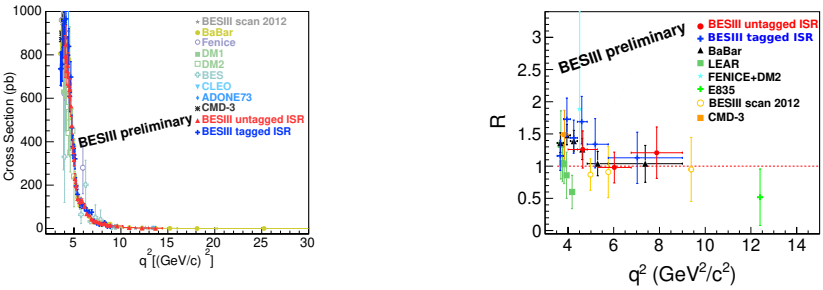

Figure 2. left: $e^+e^- \to p\bar{p}$ Born cross section results from BESIII scan [19] (grey stars), previous measurements, and the preliminary results of the BESIII ISR analyses using the tagged (blue) and untagged (red) method. **right:** Proton EMFF ratio results from BESIII scan [19] (yellow open circles), previous measurements, and the preliminary results of the BESIII ISR analyses using the tagged (blue) and untagged (red) method.

Both the tagged and untagged result of the effective FF support the observation of structures resembling the pattern of a damped oscillation, when the FF is investigated as a function of the three-momentum of the relative motion of the protons. The pattern had been reported in the analysis of the BaBar data [20, 21] and is considered as a sign for a more complex dynamic effect, which still needs clarification.

4.2 Hyperon form factors

Compared to nucleons, the hyperon EMFF are less well investigated experimentally. Thus, the BESIII data of the 2012 energy scan have also been used to study the Λ cross section and EMFF [22]. The data taken at $\sqrt{s} = 2.2324\,\text{GeV}, 2.4\,\text{GeV}, 2.8\,\text{GeV}$, and $3.08\,\text{GeV}$ allow to put emphasis on the threshold region, with the first data point being only 1 MeV above the $\Lambda\bar{\Lambda}$ threshold. The hyperons are generally reconstructed from their decay to $p\pi$. Only at threshold another strategy is necessary, since the low energetic nucleons from the decay are already stopped in the beam pipe. Here, the decay mode $n\pi^0$ is exploited in addition, and the annihilation vertices of $\bar{p}$ and $\bar{n}$ at the beam pipe are used to tag the decay of $\bar{\Lambda}$. Based on this strategy, the cross section of $\Lambda\bar{\Lambda}$ production and the effective FF have been determined. The results, illustrated in Fig. 3 are consistent with previous measurements, however, with improved accuracy. In contrast to the expectation of a vanishing cross section at threshold, the BESIII result reveals a steep increase, which hints at a more complex underlying physics scenario, requiring further detailed studies of hyperon production.

As a part of these studies a new high statistics energy scan has been carried out at BESIII in 2015. A data set of $66.9\,\text{pb}^{-1}$ at $\sqrt{s} = 2.396\,\text{GeV}$ has been acquired, aiming at the determination of the FF ratio as well as the relative phase of the EMFF of Λ. The hyperon pairs are exclusively reconstructed in the final state $e^+e^- \to \Lambda\bar{\Lambda} \to p\bar{p}\pi^+\pi^-$. Protons and pions can be identified by their different momenta. The preliminary results of the extracted cross section and effective FF are consistent with previous measurements, including the BESIII results [22]. The EMFF ratio R and the relative phase $\Delta\Phi$ are determined following the approach suggested by Fäldt and Kupść [23]. The decay distributions of the complete final state are described by a set of six functions $\mathcal{T}_i(\xi)$, where $\xi = (\theta, \theta_1, \phi_1, \theta_2, \phi_2)$ is state vector of the events, containing the scattering angle θ of the hyperon, and the decay angles θ_i and ϕ_i of the respective pair of daughter particles. The free parameters in the approach

are $\eta = \frac{\tau - R^2}{\tau + R^2}$, related to the EMFF ratio, and the relative phase $\Delta\Phi$. They are determined by performing an unbinned maximum likelihood fit to the data. The preliminary results are $R = 0.94 \pm 0.16_{\text{stat}} \pm 0.03_{\text{syst}} \pm 0.02_{\alpha_\Lambda}$ and $|\Delta\Phi| = 42^\circ \pm 16^\circ_{\text{stat}} \pm 8^\circ_{\text{syst}} \pm 6^\circ_{\alpha_\Lambda}$, where the third uncertainty reflects the deviation of the recent determination of the Λ decay constant [24] from the PDG value [25]. This is the first measurement of the relative phase of hyperon EMFF in e^+e^- collisions.

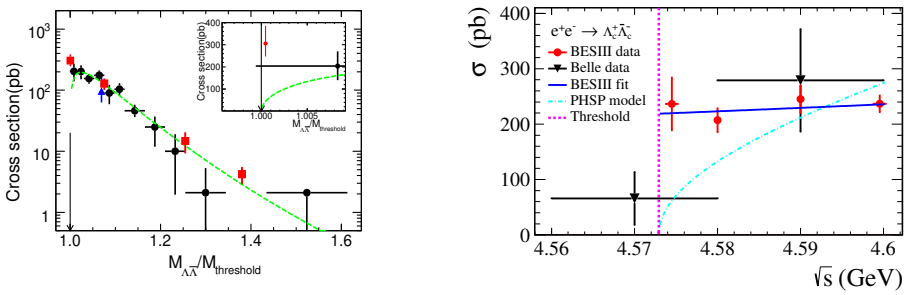

Figure 3. left: (From Ref. [22]) The Born cross section of $e^+e^- \to \Lambda\bar{\Lambda}$ from BESIII (red), BaBar (black) and DM2 (blue). The green line shows a fit with a pQCD prediction. **right:** (From Ref. [26]) The Born cross section of $e^+e^- \to \Lambda_c^+\bar{\Lambda}_c^-$ from BESIII (red) and Belle (black).

The center-of-mass energies accessible at BESIII barely allow to study the threshold region of the charmed hyperon Λ_c. The reaction $e^+e^- \to \Lambda_c^+\bar{\Lambda}_c^-$ has been studied at the four energies $\sqrt{s} = 4.5745\,\text{GeV}, 4.580\,\text{GeV}, 4.590\,\text{GeV}$ and $4.5995\,\text{GeV}$ [26]. The hyperons are reconstructed from ten Cabbibo-favored decay modes. The result cross sections are determined as the weighted average of the individual decay mode analyses. In addition to the Born cross section and the effective FF, the statistics at $\sqrt{s} = 4.5745\,\text{GeV}$ and $4.5995\,\text{GeV}$ is sufficient to determine the FF ratio in an angular analysis of the differential cross section, which is the first determination of the FF ratios for charmed baryons. As can be seen in Fig. 3, there seems to be a tension between the results for the effective FF obtained by the Belle collaboration [27] and the BESIII result. While the Belle measurement is compatible with a vanishing cross section at threshold, the BESIII result suggests a plateau in the cross section. However, the binning of the Belle result, which was obtained using the ISR method, is rather coarse. The lowest mass bin also extends below the $\Lambda_c\bar{\Lambda}_c$ threshold, which might distort the distribution. Further, high precision measurement are necessary to improve the understanding of charmed hyperon production at threshold.

5 Summary and outlook

Form factors are an essential tool to understand the structure and dynamics of hadrons in the non-perturbative regime. The BESIII experiment can exploit the methods of the conventional energy scan as well as the tagged and untagged ISR techniques to provide valuable data, which allow to gain deeper insights.

The measurement of the pion form factor with sub-percent accuracy is an important input to the calculation of the hadronic contributions to the anomalous magnetic moment of the muon a_μ. Additional investigations of higher pion multiplicities, e.g. $e^+e^- \to \pi^+\pi^-\pi^0$ and $e^+e^- \to \pi^+\pi^-\pi^0\pi^0$, which are important to further reduce the theoretical uncertainty of a_μ, are in preparation and results will be published soon.

The investigations of the nucleon EMFF will be complemented by a new high statistics scan measurement, which does not only provide additional data on the proton EMFF G_E and G_M, but also the neutron EMFF are studied. The same data are also under evaluation for hyperon FF, providing more detailed information for Λ, Σ^0, and $\Sigma^\pm$ EMFF.

Studies of the charmed hyperon EMFF at BESIII are currently limited by the accessible center-of-mass energies of the BEPCII accelerator. A possible upgrade of the machine is under investigation. The goal is to push the accessible energy range to $\sqrt{s} = 4.9$ Gev, which allows to study charmed hyperons and their decays in more details.

References

[1] C.E. Carlson, Prog. Part. Nucl. Phys. **82**, 59 (2015), 1502.05314
[2] M. Ablikim et al. (BESIII), Nucl. Instrum. Meth. **A614**, 345 (2010), 0911.4960
[3] C. Yu et al., *BEPCII Performance and Beam Dynamics Studies on Luminosity*, in *Proceedings, 7th International Particle Accelerator Conference (IPAC 2016): Busan, Korea, May 8-13, 2016* (2016), p. TUYA01
[4] X. Li et al., Radiation Detection Technology and Methods **1**, 13 (2017)
[5] Y.X. Guo et al., Radiation Detection Technology and Methods **1**, 15 (2017)
[6] M. Ablikim et al. (BESIII), Chin. Phys. **C37**, 123001 (2013), 1307.2022
[7] M. Ablikim et al. (BESIII), Chin. Phys. **C39**, 093001 (2015), 1503.03408
[8] G.W. Bennett et al. (Muon g-2), Phys. Rev. **D73**, 072003 (2006), hep-ex/0602035
[9] A. Keshavarzi, D. Nomura, T. Teubner, Phys. Rev. **D97**, 114025 (2018), 1802.02995
[10] J. Grange et al. (Muon g-2) (2015), 1501.06858
[11] T. Mibe (J-PARC g-2), Nucl. Phys. Proc. Suppl. **218**, 242 (2011)
[12] T. Blum, P.A. Boyle, V. Gulpers, T. Izubuchi, L. Jin, C. Jung, A. Juttner, C. Lehner, A. Portelli, J.T. Tsang (RBC, UKQCD), Phys. Rev. Lett. **121**, 022003 (2018), 1801.07224
[13] A. Anastasi et al. (KLOE-2), JHEP **03**, 173 (2018), 1711.03085
[14] B. Aubert et al. (BaBar), Phys. Rev. Lett. **103**, 231801 (2009), 0908.3589
[15] M. Ablikim et al. (BESIII), Phys. Lett. **B753**, 629 (2016), 1507.08188
[16] G. Rodrigo, H. Czyz, J.H. Kuhn, M. Szopa, Eur. Phys. J. **C24**, 71 (2002), hep-ph/0112184
[17] H. Czyz, J.H. Kuhn, A. Wapienik, Phys. Rev. **D77**, 114005 (2008), 0804.0359
[18] M. Davier, A. Hoecker, B. Malaescu, Z. Zhang, Eur. Phys. J. **C77**, 827 (2017), 1706.09436
[19] M. Ablikim et al. (BESIII), Phys. Rev. **D91**, 112004 (2015), 1504.02680
[20] A. Bianconi, E. Tomasi-Gustafsson, Phys. Rev. Lett. **114**, 232301 (2015), 1503.02140
[21] A. Bianconi, E. Tomasi-Gustafsson, Phys. Rev. **C93**, 035201 (2016), 1510.06338
[22] M. Ablikim et al. (BESIII), Phys. Rev. **D97**, 032013 (2018), 1709.10236
[23] G. Faldt, A. Kupsc, Phys. Lett. **B772**, 16 (2017), 1702.07288
[24] M. Ablikim et al. (BESIII) (2018), 1808.08917
[25] C. Patrignani et al. (Particle Data Group), Chin. Phys. **C40**, 100001 (2016)
[26] M. Ablikim et al. (BESIII), Phys. Rev. Lett. **120**, 132001 (2018), 1710.00150
[27] G. Pakhlova et al. (Belle), Phys. Rev. Lett. **101**, 172001 (2008), 0807.4458